HHS Public Access

Author manuscript

Science. Author manuscript; available in PMC 2019 October 25.

Published in final edited form as:

Science. 2018 November 16; 362(6416): 799–804. doi:10.1126/science.aas8961.

Heterobiaryl synthesis by contractive C-C coupling via P(V) intermediates

Michael C. Hilton[1], **Xuan Zhang**[1,*], **Benjamin T. Boyle**[1,*], **Juan V. Alegre-Requena**[1], **Robert S. Paton**[1,2,†], **Andrew McNally**[1,†]

[1]Department of Chemistry, Colorado State University, Fort Collins, CO 80523, USA.

[2]Chemistry Research Laboratory, University of Oxford, Oxford OX1 3TA, UK.

Abstract

Heterobiaryls composed of pyridine and diazine rings are key components of pharmaceuticals and are often central to pharmacological function. We present an alternative approach to metal-catalyzed cross-coupling to make heterobiaryls using contractive phosphorus C–C couplings, also termed phosphorus ligand coupling reactions. The process starts by regioselective phosphorus substitution of the C–H bonds para to nitrogen in two successive heterocycles; ligand coupling is then triggered via acidic alcohol solutions to form the heterobiaryl bond. Mechanistic studies imply that ligand coupling is an asynchronous process involving migration of one heterocycle to the ipso position of the other around a central pentacoordinate P(V) atom. The strategy can be applied to complex drug-like molecules containing multiple reactive sites and polar functional groups, and also enables convergent coupling of drug fragments and late-stage heteroarylation of pharmaceuticals.

Reactions that couple two aromatic rings to make biaryls are among the most widely used processes in the pharmaceutical industry (1, 2). Coupling of pyridines and diazines results in heterobiaryls, a privileged pharmacophore found in commercial drugs as well as numerous therapeutic candidates, such as the examples shown in Fig. 1A (3–5). These heterocycles often play a key role in drug-receptor binding and impart other important properties such as net polarity, aqueous solubility, and resistance to oxidative metabolism. Most conceivable aryl-aryl couplings can be accomplished using metal-catalyzed cross-coupling reactions;

†Corresponding author. robert.paton@chem.ox.ac.uk (R.S.P.); andy.mcnally@colostate.edu (A.M.).
*These authors contributed equally to this work.

Author contributions: M.C.H., X.Z., and B.T.B. performed the experimental work; the computational studies were performed by J.V.A.-R. and R.S.P.; all authors contributed to the design of the experimental and computational work and to data analysis, discussed the results, and commented on the manuscript; and A.M. and R.S.P. wrote the manuscript.

Competing interests: The authors declare no competing interests;

Data and materials availability: All data are available in the main text or the supplementary materials.

SUPPLEMENTARY MATERIALS

www.sciencemag.org/content/362/6416/799/suppl/DC1

Materials and Methods
Figs. S1 to S26
Tables S1 to S22
NMR Spectra
References (44–97)
Movies S1 and S2

these processes feature exceptional chemoselectivity, precise regioselectivity, and sufficient robustness to be applied to both drug discovery and manufacture (6–8). However, the same synthetic prowess is not transferable to heteroarylheteroaryl coupling, particularly for complex substrates. An alternative strategy that addresses the shortcomings in this fundamental bond construction would therefore offer new opportunities to incorporate heterobiaryls into therapeutic candidates.

For de novo synthesis of heterobiaryls, a schematic for metal-catalyzed cross-couplings is shown in Fig. 1B (9–15). A minimum of three steps are required, and there are challenges in the coupling step, such as catalyst poisoning and decomposition of starting materials (16). Furthermore, drug-like molecules and intermediates often have multiple reactive sites and a high proportion of polar functional groups, such as basic amines, that interfere with catalytic processes and cause a considerable number of them to fail (15, 17). Another serious problem arises from the lack of methods to prepare the cross-coupling precursors. Although simple heteroaryl halides are commercially available or can be straightforwardly prepared, direct and selective halogenation of pyridine and diazine derivatives encountered during drug development remains an unsolved challenge (18, 19). Similarly, synthesizing nucleophilic coupling partners such as heteroaryl boronic acids, stannanes, and organozinc or magnesium compounds is challenging, and they are often prepared from the corresponding heteroaryl halides to begin with (20). Cross-dehydrogenative couplings of heteroarenes have shown some promise but are currently limited to specific pyridine combinations and are not applicable in complex settings (21).

Reaction development

The limitations of current heterocycle coupling methods can potentially be overcome by contractive phosphorus C−C couplings, often termed phosphorus ligand coupling reactions; a test system is shown in Fig. 1C (22–24). The strategy does not rely on heteroaryl halides or partners such as boronic acids, but instead regioselectively substitutes the C−H bond in each heterocyclic coupling partner by successive C−P bond formations to produce a bis-azaarene phosphonium salt; phosphorus ligand coupling is then triggered to form the heterobiaryl bond via a P(V) intermediate. Heteroaryl-heteroaryl coupling has previously been observed at phosphorus centers, but an inability to transform a generic set of pyridines and diazine precursors into the required bis-azaarene phosphonium salts has restricted these processes to specialized cases (25–29). In our test system, stage A combined the first heterocycle, 2-phenylpyridine, with Tf_2O at low temperature to form an intermediate pyridinium triflyl salt (not shown); adding fragmentable phosphine **1** (prepared on large scale from diphenyl phosphine and methyl acrylate) (30) results in a para-selective reaction to form dearomatized intermediate **Int-I** (31–37). Two equivalents of DBU (1,8-diazabicyclo[5.4.0]undec-7-ene) eliminate first the triflyl anion to form phosphonium ion **Int-II**, and then methyl acrylate to form heteroaryl phosphine **2a** in good yield. Pyridine was chosen as the second coupling partner in stage B with phosphine **2a** as a nucleophile, resulting in bis-heteroaryl phosphonium salt **3a**, with complete regiocontrol. Several nucleophiles are known to initiate phosphorus ligand coupling, including alkoxides, Grignard reagents, and acidic alcohol solutions (22, 25–29); for stage C, we found the latter to be most effective and two equivalents of HCl in EtOH at 80°C to be optimal, forming heterobiaryl **4a** in excellent yield

with diphenylphosphine oxide as a by-product (see table S1). We did not observe products from heteroaryl-phenyl or phenyl-phenyl coupling, nor ethoxylation of either heterocycle, in this protocol.

Mechanistic investigation

To investigate the reasons for selective heterocycle-heterocycle coupling and the kinetics of the ligand-coupling process, we performed a series of experimental and computational studies. We hypothesized that ethanol attacks the phosphorus center and a P(V) species is formed. Subjecting salt **3a** to a solution of DCl in d_4-methanol results in successive shifts of pyridine proton resonances per equivalent of acid by ^{1}H NMR (nuclear magnetic resonance) and ^{31}P NMR spectroscopy, and indicates that both pyridines are protonated (see figs. S17 and S18). However, no P(V) intermediates were detected in a ^{31}P NMR study under the reaction conditions. Computational studies do predict that intramolecular ligand coupling occurs from P(V) intermediate **Int-III** in a stepwise fashion (see below) and that there is a substantial barrier-lowering effect ($\Delta G^{\ddagger}$) upon successive protonation of **Int-III** (Fig. 2A) (38). Transition state energies considerably favor pyridine-pyridine coupling over pyridine-phenyl coupling for each protonation state; ΔG^{react} values show that the process is similarly exergonic and irreversible in each case, reinforcing the conclusion that selective pyridine-pyridine coupling results from kinetic differences in the ligand-coupling transition state rather than thermodynamic factors. The intrinsic reaction co-ordinate (IRC; Fig. 2B) shows no involvement of alkoxy lone pairs and negligible changes to the other three equatorial P−C bonds. In the C−C bond-forming transition structure [**TS-I·2H**]$^{2+}$, a single P−C bond breaks, allowing one ligand to migrate to the ipso-carbon of another (Fig. 2C). The intermediate formed in this key step ([**Int-IV·2H**]$^{2+}$) is a dearomatized adduct characteristic of nucleophilic aromatic substitution, which is predicted to collapse irreversibly (ΔG = −39 kcal/mol) and with considerable ease (see figs. S9 to S11). This stepwise ligand coupling is therefore mechanistically distinct from the concerted cleavage of two σ-bonds during reductive elimination at, for example, Pd(II) or in dihydrogen formation from PH_5. This latter detail is important because concerted coupling of apical-equatorial substituents from a (D_{3h}) trigonal bipyramidal compound is symmetry-forbidden (fig. S6) (24): in contrast, this stepwise-coupling mechanism permits, and indeed favors, the migration of an apical ligand to an equatorial one ([**TS-I·2H**]$^{2+}$) (fig. S7).

The computed structures of P(V) intermediates, such as [**Int-III·2H**]$^{2+}$, are characterized by stronger, shorter ($d_{\text{P–C(py)}}$ = 1.86 Å) bonds to equatorial ligands and weaker, longer ($d_{\text{P–C(py)}}$ = 1.99 Å) bonds to those in apical positions. This is a result of three-center, four-electron bonding between the apical ligands and the central phosphorus atom. Accordingly, the relative stability of P(V) stereoisomeric forms can be readily predicted on the basis of each ligand's capacity to stabilize the buildup of electron density at the apical positions: σ-electron–withdrawing alkoxy and heteroaryl groups preferentially occupy the apical sites (fig. S5). Weaker and more polar apical P−L bonds favor migration in nucleophilic 1,2-rearrangements, in which an equatorial ligand acts as the electrophilic acceptor (fig. S7), leading to ligand coupling. Phenyl ligands are unfavorable for both donor and acceptor roles in ligand coupling: Apical positions (donors) favor more σ-electron–withdrawing substituents, whereas pyridyl substituents are superior acceptors. This explains the complete

absence of bi-phenyl and phenyl-heterobiaryl coupled products. N-protonation decreases the activation barrier considerably, from 30 to 20 kcal/mol, increasing the electrophilicity of the equatorial pyridyl group. Successive N-protonation further reduces the activation barrier to 14 kcal/mol by increasing the σ-electron–withdrawing power of the axial donor ligand and weakening the P−C bond ($d_{P-C(py)}$ increases from 1.95 Å in [**Int-III·H**]$^{+}$ to 1.99 Å in [**Int-III·2H**]$^{2+}$), whereas equatorial P−C bonds are largely unchanged ($d_{P-C(py)}$ is 1.87 Å in [**Int-III·H**]$^{+}$ and 1.86 Å in [**Int-III·2H**]$^{2+}$). Computed values of C−O coupling from **Int-**[**Int-III·2H**]$^{2+}$ are also disfavored relative to pyridine-pyridine coupling ($\Delta G^{\ddagger(C-O)}$ = 18 kcal/mol versus $\Delta G^{\ddagger(py\text{-}py)}$ = 14 kcal/mol; fig. S8) (31).

Figure 2D examines the effect of phosphorus electrophilicity on the rate of heterobiaryl formation. The low energy barrier for ligand coupling in [**Int-III·2H**]$^{2+}$ implies that the rate-determining step precedes this event and involves attack of the alcoholic solvent at the phosphonium center. We prepared a set of salts with substituted aryl groups that would change the electrophilicity at phosphorus; rate data show faster heterobiaryl formation as the electrophilicity of the phosphonium increases, in line with the above hypothesis. Further experimental verification of the low barriers for ligand coupling is shown in Fig. 2E. Acidic alcohol solutions are inefficient for heterobiaryl formation at lower temperatures (table S1); however, when ethoxide is used as a nucleophile for facile addition to the phosphonium ion (fig. S24), heterobiaryl synthesis occurs in minutes at room temperature, with trace amounts of C−O coupling also observed. Substantial amounts of products resulting from protiodephosphination are formed under these conditions, making this protocol less practical than that under acidic conditions.

Substrate scope exploration

We next selected a set of pyridines and diazines to examine which substitution patterns and functional groups could be tolerated in the ligand coupling process (Fig. 3). The reaction is completely selective for the 4-position of pyridines in the vast majority of cases studied, unless a 4-substituent is present, which switches selectivity to the 2-position. A variety of 4,4′-bipyridines are accessible using this strategy (**4b–4f**); functional groups such as esters, trifluoromethyl groups, and methoxy groups are accommodated, as are halides that would normally be active in metal-catalyzed reactions. Substituents can be present at the 2- or 3-positions of pyridines, and example **4e** shows that a 2-position substituent is not a requirement (see below). A fluorinated 2,4′-quinoline-pyridine was also synthesized by phosphorus ligand coupling (**4g**) (39). Examples of 2,2′-systems, **4h** and **4i**, showcase an alternative to Suzuki couplings, where 2-pyridyl and quinolyl boronic acids often decompose during metal-catalyzed reactions (16). Pyrimidine- and pyrazine-containing heterobiaryls **4j** and **4k** were formed via the three-step sequence, with lower yields in the coupling step relative to pyridine examples.

Reaction guidelines

During these studies, we have established a general set of reaction guidelines and limitations. First, when coupling 2-substituted pyridines to 3-substituted pyridines, it is important to perform the salt-forming sequence in the correct order (Fig. 3). Taking

heterobiaryl **4b** as a representative example, if heteroaryl phosphine **2b′** is used instead in stage B, then salt **3b** is not formed. We believe that a biased Tf-salt equilibrium rapidly develops, and pyridinium-phosphine [**2b′-Tf**]$^+$ is favored on steric grounds; the 2-substituted pyridine is then not activated for nucleophilic addition, and the desired salt is not formed (fig. S25). Instead, the 2-substituted pyridine should be converted into the corresponding phosphine and used as a nucleophile with the 3-substituted pyridine in stage B. Second, problematic substrates for heteroaryl phosphine and salt formation include pyridines with 2-trifluoromethyl groups, 4-alkyl or aryl substituents, and 2,6-disubstituted pyridines. In general, pyridines and diazines with more than two electron-withdrawing groups or electron-donating groups can result in low yields or no phosphonium salt formation. During ligand coupling, we have observed that pyridines substituted with bromides and iodides can be dehalogenated, that 2-chloro- or 2-fluoropyridines are not successful, and that 2-methoxypyridines proceed with slower rates. For pyridines containing electron-withdrawing groups, using EtOH and HCl can result in ethoxylation. Changing the acid to TfOH avoids this problem and leads us to believe that ethoxylation results from chlorination followed by ethoxylation via nucleophilic aromatic substitution. Trifluoroethanol is preferred when molecules contain functional groups such as amides and esters that are susceptible to ethanolysis. In general, one equivalent of acid per basic nitrogen is optimal (see below).

Application to complex intermediates

Our attention then turned to ligand couplings involving complex azaarenes (Fig. 4). Convergent couplings of pyridine-containing fragments were first examined; these molecules are representative of drug leads, which are promising candidates for a therapeutic target but have suboptimal pharmacokinetic and pharmacodynamic properties (40). A convergent coupling strategy would enable rapid access to complex heterobiaryls from compounds common in pharmaceutical libraries (41, 42). Four examples in Fig. 4 are shown where the corresponding halide precursors are not commercially available or would be challenging to prepare (**4l–4o**). Heterobiaryl bonds are formed with precise regioselectivity, and the presence of additional saturated and unsaturated nitrogen heterocycles is tolerated in this approach. Three or four equivalents of acid are used in the coupling step in these cases to ensure adequate reaction rates.

Next, we investigated whether the ligand-coupling strategy could be applied to advanced intermediates in drug development. Success in this endeavor would offer distinct strategies to introduce heterobiaryls into complex molecules and alleviate concerns over metal contamination in subsequent biological testing. To demonstrate the feasibility of this approach, we chose a set of existing drug molecules with diverse structures, substitution patterns, and functional groups (43).

The use of previously synthesized heteroaryl phosphines (Fig. 4) shows that heteroarylation is possible in these complex systems with complete control of regioselectivity and site selectivity. Chlorphenamine, a common antihistamine, and loratadine, an allergy medicine, are competent substrates for this protocol, with the resulting heterobiaryls isolated in good overall yields (**4p** and **4q**) that again highlight how halides can be tolerated during the

coupling procedure. Vismodegib was converted into a 2,4′-quinoline-pyridine system in moderate yield (**4r**). A widely applied fungicide, quinoxyfen, was also compatible with the reaction protocol (**4s**). Etoricoxib and imatinib are challenging examples because they contain multiple reactive sites (34). The structural features in etoricoxib enable selective transformation of the 2,5-disubstituted pyridine (**4t**), and heteroarylation of the pyridine occurs selectively over the pyrimidine in imatinib to form **4u**.

Outlook

This phosphorus ligand coupling method over-comes major limitations of metal-catalyzed approaches by virtue of its compatibility with polar functionalities found in drug-like molecules and its circumvention of preformed heteroaryl halides and boronic acids. As well as transforming building block compounds, convergent coupling of drug fragments and heteroarylation of complex pharmaceuticals were demonstrated. The protocol uses readily available reagents under simple conditions and is immediately applicable in medicinal chemistry.

Supplementary Material

Refer to Web version on PubMed Central for supplementary material.

ACKNOWLEDGMENTS

Funding: Supported by startup funds from Colorado State University and by NIH award R01 GM124094–01 (A.M., M.C.H., X.Z., and B.T.B.). We acknowledge the RMACC Summit supercomputer, supported by NSF grants ACI-1532235 and ACI-1532236, the University of Colorado Boulder, Colorado State University, and the Extreme Science and Engineering Discovery Environment (XSEDE) through allocations TG-CHE180006 and TG-CHE180056. XSEDE is supported by NSF grant ACI-1548562.

REFERENCES AND NOTES

1. Brown DG, Boström J, J. Med. Chem 59, 4443–4458 (2016). [PubMed: 26571338]
2. Roughley SD, Jordan AM, J. Med. Chem 54, 3451–3479 (2011). [PubMed: 21504168]
3. Capdeville R, Buchdunger E, Zimmermann J, Matter A, Nat. Rev. Drug Discov 1, 493–502 (2002). [PubMed: 12120256]
4. Roecker AJ et al., ChemMedChem 9, 311–322 (2014). [PubMed: 24376006]
5. Martina SD, Vesta KS, Ripley TL, Ann. Pharmacother 39, 854–862 (2005). [PubMed: 15827069]
6. Crawley ML, Trost BM, Applications of Transition Metal Catalysts in Drug Discovery and Development: An Industrial Perspective (Wiley, 2012), pp. 25–96.
7. de Meijere A, Diederich F, Metal-Catalyzed Cross-Coupling Reactions (Wiley-VCH, ed. 2, 2004).
8. Hassan J, Sévignon M, Gozzi C, Schulz E, Lemaire M, Chem. Rev 102, 1359–1470 (2002). [PubMed: 11996540]
9. Campeau L-C, Fagnou K, Chem. Soc. Rev 36, 1058–1068 (2007). [PubMed: 17576474]
10. Zhao D, You J, Hu C, Chem. Eur. J 17, 5466–5492 (2011). [PubMed: 21506178]
11. Billingsley KL, Anderson KW, Buchwald SL, Angew. Chem. Int. Ed 45, 3484–3488 (2006).
12. Kudo N, Perseghini M, Fu GC, Angew. Chem. Int. Ed 45, 1282–1284 (2006).
13. Guram AS et al., J. Org. Chem 72, 5104–5112 (2007). [PubMed: 17550290]
14. Kiehne U, Bunzen J, Lützen A, Synthesis 1061–1069 (2007).
15. Markovic T, Rocke BN, Blakemore DC, Mascitti V, Willis MC, Chem. Sci 8, 4437–4442 (2017). [PubMed: 28936330]

16. Cox PA et al., J. Am. Chem. Soc 139, 13156–13165 (2017). [PubMed: 28823150]
17. Blakemore DC et al., Nat. Chem 10, 383–394 (2018). [PubMed: 29568051]
18. Joule JA, Mills K, Heterocyclic Chemistry (Wiley-Blackwell, ed. 5, 2013).
19. Grimmett MR, Adv. Heterocycl. Chem 58, 271–345 (1993).
20. Larsen MA, Hartwig JF, J. Am. Chem. Soc 136, 4287–4299 (2014). [PubMed: 24506058]
21. Do H-Q, Daugulis O, J. Am. Chem. Soc 133, 13577–13586 (2011). [PubMed: 21823581]
22. Finer J-P, in Ligand Coupling Reactions with Heteroaromatic Compounds, Vol. 18 (Pergamon, 1998), chap. 4.
23. Reichl KD, Radosevich AT, Chem. Commun 50, 9302–9305 (2014).
24. Hoffmann R, Howell JM, Muetterties EL, J. Am. Chem. Soc 94, 3047–3058 (1972).
25. Mann FG, Watson J, J. Org. Chem 13, 502–531 (1948).
26. Newkome GR, Hager DC, J. Am. Chem. Soc 100, 5567–5568 (1978).
27. Uchida Y, Onoue K, Tada N, Nagao F, Oae S, Tetrahedron Lett. 30, 567–570 (1989).
28. Uchida Y, Kozawa H, Oae S, Tetrahedron Lett. 30, 6365–6368 (1989).
29. Uchida Y, Echikawa N, Oae S, Heteroatom Chem. 5, 409–413 (1994).
30. Alonso F, Moglie Y, Radivoy G, Yus M, Green Chem. 14, 2699–2702 (2012).
31. Hilton MC, Dolewski RD, McNally A, J. Am. Chem. Soc 138, 13806–13809 (2016). [PubMed: 27731999]
32. Zhang X, McNally A, Angew. Chem. Int. Ed 56, 9833–9836 (2017).
33. Koniarczyk JL, Hesk D, Overgard A, Davies IW, McNally A, J. Am. Chem. Soc 140, 1990–1993 (2018). [PubMed: 29377684]
34. Dolewski RD, Fricke PJ, McNally A, J. Am. Chem. Soc 140, 8020–8026 (2018). [PubMed: 29792698]
35. Anderson RG, Jett BM, McNally A, Angew. Chem. Int. Ed 57, 12514–12518 (2018).
36. Anders E, Markus F, Tetrahedron Lett. 28, 2675–2676 (1987).
37. Fier PS, J. Am. Chem. Soc 139, 9499–9502 (2017). [PubMed: 28677963]
38. Both DLPNO-CCSD(T)/cc-pV(DT)Z and wB97XD/def2-QZVPP results are in close-agreement. Full details in the supplementary materials.
39. Afzal O et al., Eur. J. Med. Chem 97, 871–910 (2015). [PubMed: 25073919]
40. Silverman RB, Holladay MW, in The Organic Chemistry of Drug Design and Drug Action (Academic Press, ed. 3, 2014), chap. 2.
41. Erlanson DA, Fesik SW, Hubbard RE, Jahnke W, Jhoti H, Nat. Rev. Drug Discov 15, 605–619 (2016). [PubMed: 27417849]
42. Murray CW, Rees DC, Nat. Chem 1, 187–192 (2009). [PubMed: 21378847]
43. Cernak T, Dykstra KD, Tyagarajan S, Vachal P, Krska SW, Chem. Soc. Rev 45, 546–576 (2016). [PubMed: 26507237]

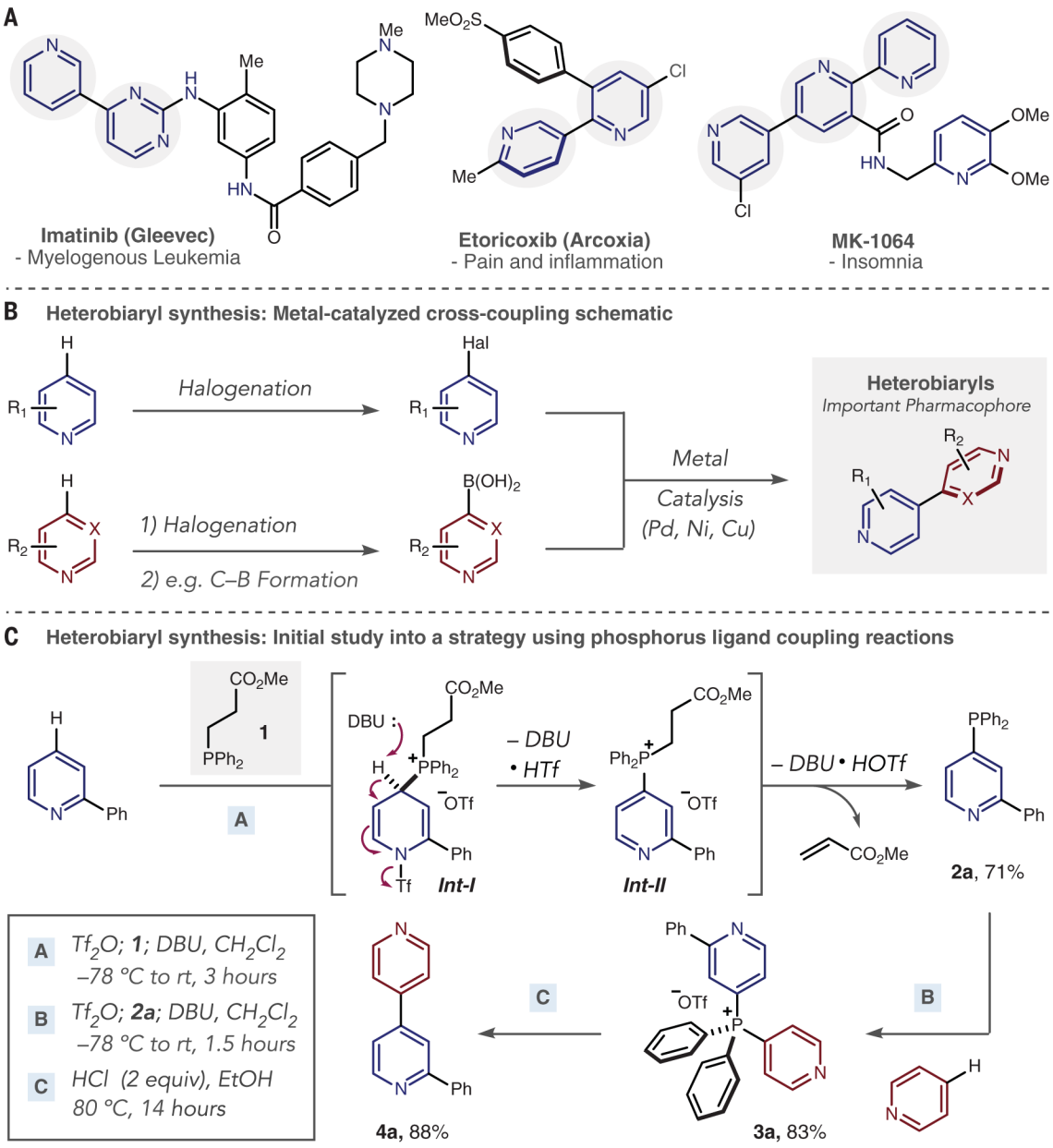

Fig. 1. Important heterobiaryl-containing drugs and synthetic strategies.

(**A**) Heterobiaryls in drugs. (**B**) Heterobiaryls via metal-catalyzed cross-coupling reactions. R denotes a general organic group; Hal, halogen substituent. (**C**) Test system for heterobiaryl synthesis via phosphorus ligand coupling reactions. Ph, phenyl; Me, methyl; Et, ethyl; Tf, trifluoromethylsulfonyl; DBU, 1,8-diazabicyclo[5.4.0] undec-7-ene; rt, room temperature.

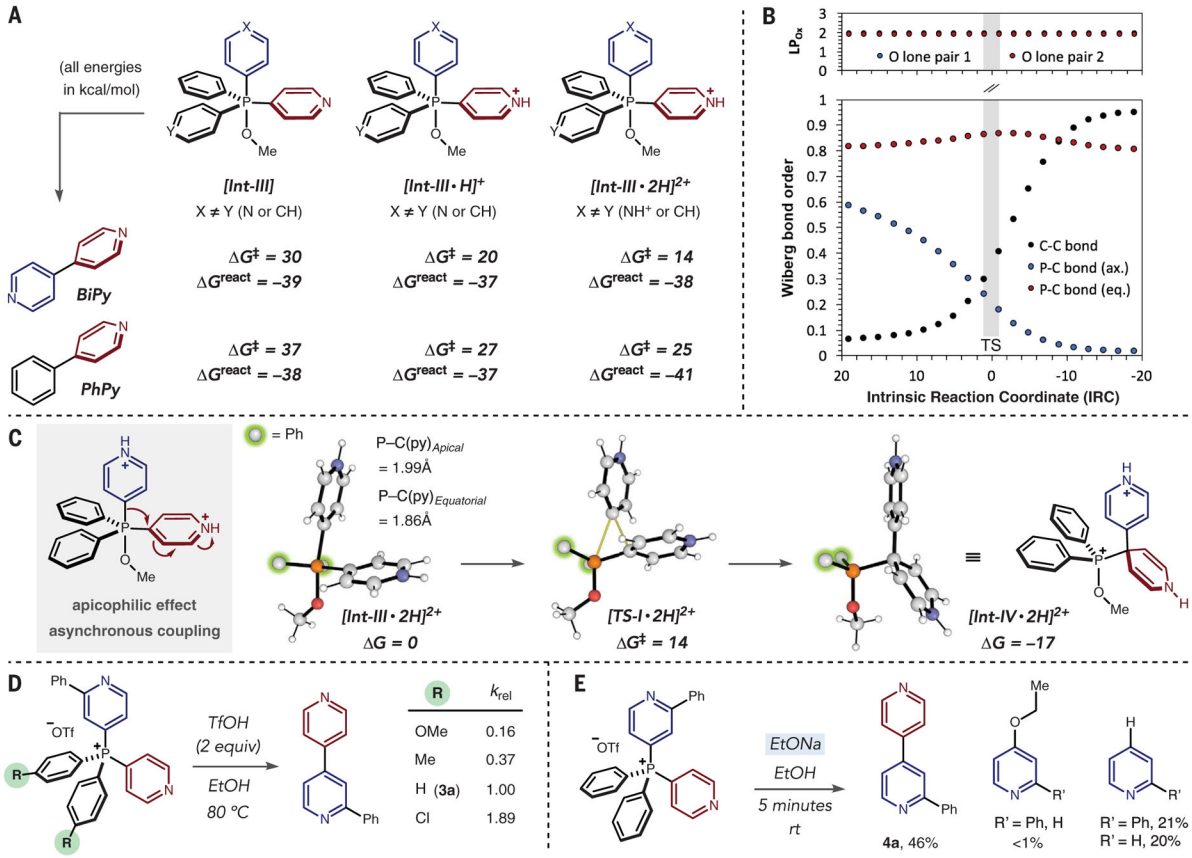

Fig. 2. Computational and experimental investigation of phosphorus ligand coupling.

(**A**) Biaryl-coupling activation barriers [coupled cluster/density functional theory SMD-DLPNO-CCSD(T)/cc-pV(DT)Z//ωB97XD/6–31+G(d), kcal/mol] decrease upon protonation and consistently favor heterobiaryl formation. Py, pyridine. (**B**) Computed bond orders show a single (apical) P−C(py) bond breaking along the reaction coordinate, with little involvement of oxygen lone pairs. LP_{Ox}, number of electrons in each oxygen lone pair. (**C**) Optimized structures for [**Int-III·2H**]$^{2+}$, [**TS-I·2H**]$^{2+}$, and [**Int-IV·2H**]$^{2+}$ show stepwise apical-equatorial ligand coupling. (**D**) A kinetic study indicates that alcohol addition is rate-limiting. TfOH was used in place of HCl because of poor solubility of aryl derivatives. Yields after complete consumption of the phosphonium salts were approximately the same in each case (89 to 94%). (**E**) Room-temperature coupling using ethoxide as a nucleophile.

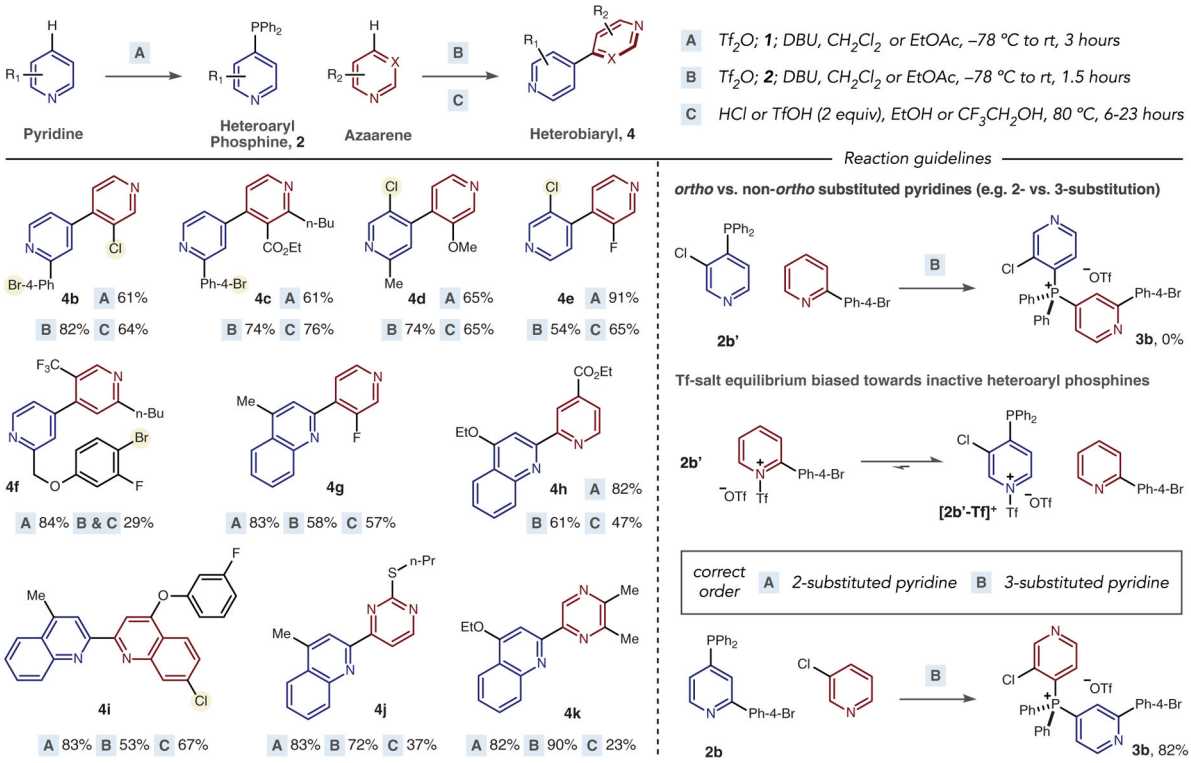

Fig. 3. Azaarene scope and guidelines for phosphonium salt formation.

Yields of isolated products after each stage are shown. *n*-Bu, normal butyl group; *n*-Pr, normal propyl group. Reaction guidelines are shown for phosphonium salt formation involving ortho and non-ortho substituted pyridines as partners. Further details of challenges and limitations are highlighted in fig. S25.

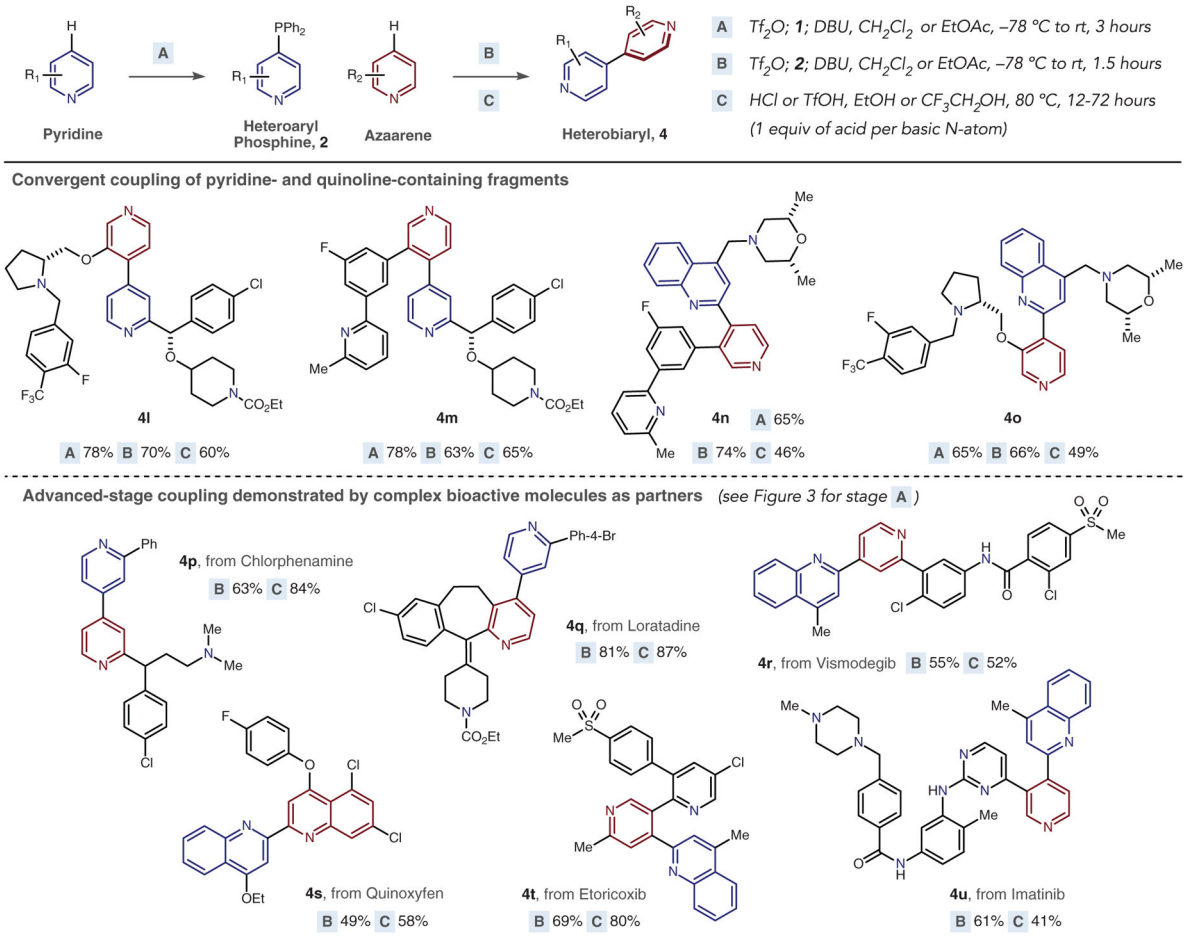

Fig. 4. Heterobiaryl synthesis in complex molecules.

Yields of isolated products after each stage are shown. Further examples of advanced stage couplings are shown in fig. S26.